

Fast Multipole BEM for Structural–Acoustics Simulation

Matthias Fischer and Lothar Gaul

Institut A für Mechanik, Universität Stuttgart, Germany

Contents

- Symmetric Galerkin BEM for acoustics
- Fast multilevel multipole algorithm
- Parameter study: accuracy vs. efficiency
- Preconditioning of the multipole BEM

Acoustic behaviour is a major concern in product development.

- Noise level influences buying decision,
- legal requirements must be fulfilled,
- acoustic instabilities can cause failure.

⇒ Efficient and reliable numerical simulation tools are required

Boundary Element Method (BEM) is suitable.

- Excellent accuracy,
- easy mesh generation,
- infinite domains pose no difficulties,
- limited by fully populated matrices.

⇒ Reduction of numerical cost by Multipole BEM

A silhouette of an Airbus A340-300 aircraft is shown in flight against a clear blue sky. The sun is setting or rising behind the plane, creating a bright, golden glow and casting long, horizontal shadows of clouds across the sky. The aircraft is positioned horizontally across the middle of the frame. Two white lines point from text labels to the tail and cockpit areas of the plane.

AIRBUS

© SETTING THE STANDARDS
<http://www.airbus.com>

"Stop snoring"

"Sorry"

THE WORLD'S QUIETEST
LONG HAUL CABIN.

The Airbus A340 is an extremely private jet. A similarity it shares with the other members of our latest wide-bodied family, the A330. It affords businessmen the luxury to hear themselves think, and more importantly, to sleep. Which is why you'll also find no dreaded middle seat in business class. A fact that disturbs our competitors, not our passengers.

Helmholtz equation

$$\nabla^2 u(x) + k^2 u(x) = 0$$

in exterior domain Ω_e with boundary conditions

$$u(x) = p(x), \quad x \in \Gamma_D, \quad \frac{\partial u(x)}{\partial n} = q(x), \quad x \in \Gamma_N$$

Sommerfeld radiation condition

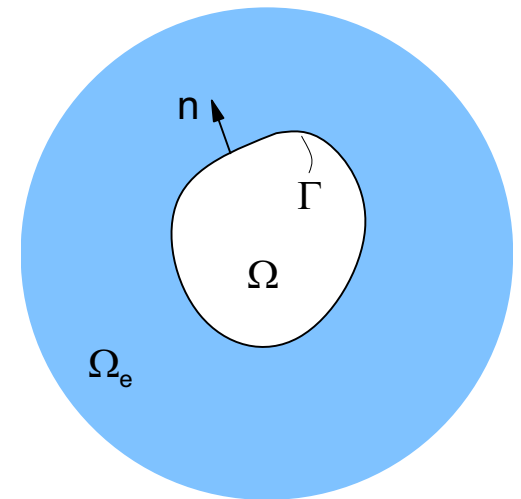
$$\left| \frac{\partial u}{\partial r} - iku \right| \leq \frac{c}{r^2} \quad \text{at } r \rightarrow \infty$$

Representation formula

$$u(y) = - \int_{\Gamma} U^*(x, y) \frac{\partial u(x)}{\partial n} ds_x + \int_{\Gamma} \frac{\partial U^*(x, y)}{\partial n_x} u(x) ds_x, \quad y \in \Omega_e$$

Fundamental solution in \mathbb{R}^3

$$U^*(x, y) = \frac{1}{4\pi} \frac{e^{ikr}}{r}$$



Limit on the smooth boundary, $\Omega_e \ni y \rightarrow \Gamma$

$$u(y) = \frac{1}{2}u(y) - \underbrace{\int_{\Gamma} U^*(x, y) \frac{\partial u(x)}{\partial n} ds_x}_{(V \partial u / \partial n)(y)} + \underbrace{\int_{\Gamma} \frac{\partial U^*(x, y)}{\partial n_x} u(x) ds_x}_{(Ku)(y)}, \quad y \in \Gamma$$

Normal derivative on the smooth boundary, $\Omega_e \ni y \rightarrow \Gamma$

$$\frac{\partial u(y)}{\partial n} = \frac{1}{2} \frac{\partial u(y)}{\partial n} - \underbrace{\int_{\Gamma} \frac{\partial U^*(x, y)}{\partial n_y} \frac{\partial u(x)}{\partial n} ds_x}_{(K' \partial u / \partial n)(y)} + \underbrace{\int_{\Gamma} \frac{\partial^2 U^*(x, y)}{\partial n_x \partial n_y} u(x) ds_x}_{-(Du)(y)}, \quad y \in \Gamma$$

Yielding the **Calderon projector**

$$\begin{pmatrix} u \\ \partial u / \partial n \end{pmatrix} = \begin{pmatrix} \frac{1}{2}I + K & -V \\ -D & \frac{1}{2}I - K' \end{pmatrix} \begin{pmatrix} u \\ \partial u / \partial n \end{pmatrix}$$

Hypersingular BIE for Neumann problem $\partial u / \partial n = q$ on Γ

$$\int_{\Gamma} \frac{\partial^2 U^*(x, y)}{\partial n_x \partial n_y} u(x) \, ds_x = \frac{1}{2} q(y) + \int_{\Gamma} \frac{\partial U^*(x, y)}{\partial n_y} q(x) \, ds_x$$

Discretization

linear shape functions for pressure $u_h = \sum_{i=1}^N \varphi_i(x) u_i$

constant shape functions for flux $q_h = \sum_{k=1}^M \psi_k(x) q_k$

Testing with linear test functions $\varphi_j(y)$

$$\begin{aligned} & \sum_{i=1}^N \left\{ \int_{\Gamma} \varphi_j(y) \int_{\Gamma} \frac{\partial^2 U^*(x, y)}{\partial n_x \partial n_y} \varphi_i(x) \, ds_x \, ds_y \right\} u_i \\ &= \sum_{k=1}^M \left\{ \int_{\Gamma} \varphi_j(y) \left(\frac{1}{2} \psi_k(y) + \int_{\Gamma} \frac{\partial U^*(x, y)}{\partial n_y} \psi_k(x) \, ds_x \right) \, ds_y \right\} q_k \quad \text{for } j = 1 \dots N \end{aligned}$$

Matrix formulation $-D_h[j, i] u_i = \left(\frac{1}{2} I_h[j, k] + K'_h[j, k] \right) q_k$

Hypersingular operator $D_h[j, i]$ is **not integrable**

$$\int_{\Gamma} \varphi_j(y) \int_{\Gamma} \frac{\partial^2 U^*(x, y)}{\partial n_x \partial n_y} \varphi_i(x) \, ds_x \, ds_y = \int_{\Gamma} \int_{\Gamma} k^2 n_x \cdot n_y \varphi_i(x) \varphi_j(y) U^*(x, y) \, ds_x \, ds_y \\ - \int_{\Gamma} \varphi_j(y) \int_{\Gamma} \varphi_i(x) n_x \cdot [\nabla_x \times (n_y \times \nabla_y U^*(x, y))] \, ds_x \, ds_y$$

Applying **Stoke's theorem** twice on second integral

$$D_h[j, i] = \int_{\Gamma} \int_{\Gamma} k^2 n_x \cdot n_y \varphi_i(x) \varphi_j(y) U^*(x, y) \, ds_x \, ds_y \\ - \int_{\Gamma} \int_{\Gamma} ((n_x \times \nabla_x \varphi_i(x)) \cdot \underbrace{(n_y \times \nabla_y \varphi_j(y))}_{\text{curl}_{\Gamma}(\varphi_j)}) U^*(x, y) \, ds_x \, ds_y$$

constant on
linear element

⇒ Hypersingular operator requires evaluation of single layer potential with constant and linear shape functions.

System matrices are fully populated

- high memory requirements, high computational cost

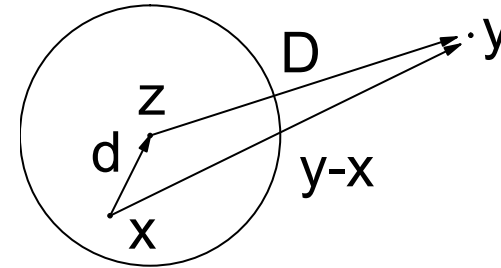
For iterative solution only the matrix-vector product must be evaluated

⇒ **Fast multipole method (FMM)** [Greengard, Rokhlin 1987]

Evaluation of $\underline{v} = V_h \underline{w}$ for the discrete single layer potential using the FMM

$$\begin{aligned}
 v_l &= \underbrace{\sum_{\text{nearfield}} V_h[l, k] w_k}_{\text{direct evaluation}} + \sum_{\text{farfield}} w_k \int_{\tau_l} \int_{\tau_k} \underbrace{U^*(x, y)}_{\text{smooth function}} ds_x ds_y \\
 &\quad \Rightarrow \text{multipole expansion} \\
 &\approx \sum_{\text{nearfield}} V_h[l, k] w_k + \sum_{j=1}^{G_l} \omega_{l,j} \Delta_l \underbrace{\sum_{\text{farfield}} w_k \sum_{i=1}^{G_k} \omega_{k,i} \Delta_k U^*(x_{k,i}, y_{l,j})}_{q_{k,i} U^*(x_{k,i}, y_{l,j})}
 \end{aligned}$$

Series expansion of fundamental solution



$$\frac{e^{ik|y-x|}}{|y-x|} = \frac{e^{ik|D+d|}}{|D+d|} = ik \sum_{l=0}^{\infty} (2l+1) j_l(kd) h_l^{(1)}(kD) P_l(\hat{D} \cdot \hat{d}), \quad |D| > |d|$$

Orthonormality on unit sphere \mathbb{S}^2 and plane wave expansion

$$4\pi i^l j_l(kd) P_l(\hat{D} \cdot \hat{d}) = \int_{\mathbb{S}^2} e^{ikd \cdot s} P_l(s \cdot \hat{D}) ds$$

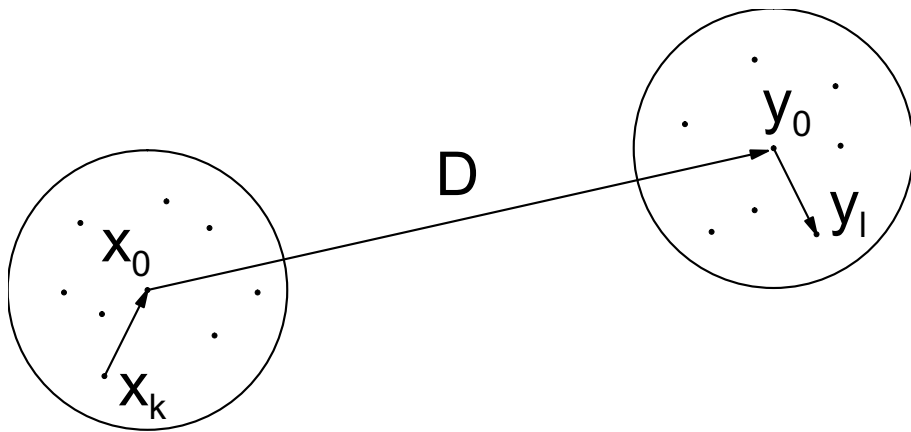
$$\Rightarrow \frac{e^{ik|D+d|}}{|D+d|} = \frac{ik}{4\pi} \sum_{l=0}^{\infty} (2l+1) i^l h_l^{(1)}(kD) \int_{\mathbb{S}^2} e^{ikd \cdot s} P_l(s \cdot \hat{D}) ds$$

Truncation of series expansion and definition of translation operators

$$M_L(s, D) = \sum_{l=0}^L (2l+1) i^l h_l^{(1)}(kD) P_l(s \cdot \hat{D})$$

Advantages of series expansion

- separation of local distance d and translation D
- diagonal form, simple translation to new expansion center



Task:

For two well-separated sets of points,

$$\{x_k\}_{k=1}^M \text{ and } \{y_l\}_{l=1}^N,$$

compute potential

$$\Phi(y_l) = \sum_{k=1}^M q_k U^*(x_k, y_l)$$

Direct evaluation: Numerical cost $\mathcal{O}(MN)$

Evaluation using translation operators

$$\Phi(y_l) = \frac{ik}{4\pi} \int_{\mathbb{S}^2} e^{ik(y_l - y_0) \cdot s} M_L(s, y_0 - x_0) \underbrace{\sum_{k=1}^M e^{ik(x_0 - x_k) \cdot s} q_k}_{\text{farfield signature } F(s)} ds.$$

\Rightarrow Numerical cost $\mathcal{O}(M) + \mathcal{O}(N)$

farfield signature $F(s)$

Further improvement of efficiency by multilevel scheme

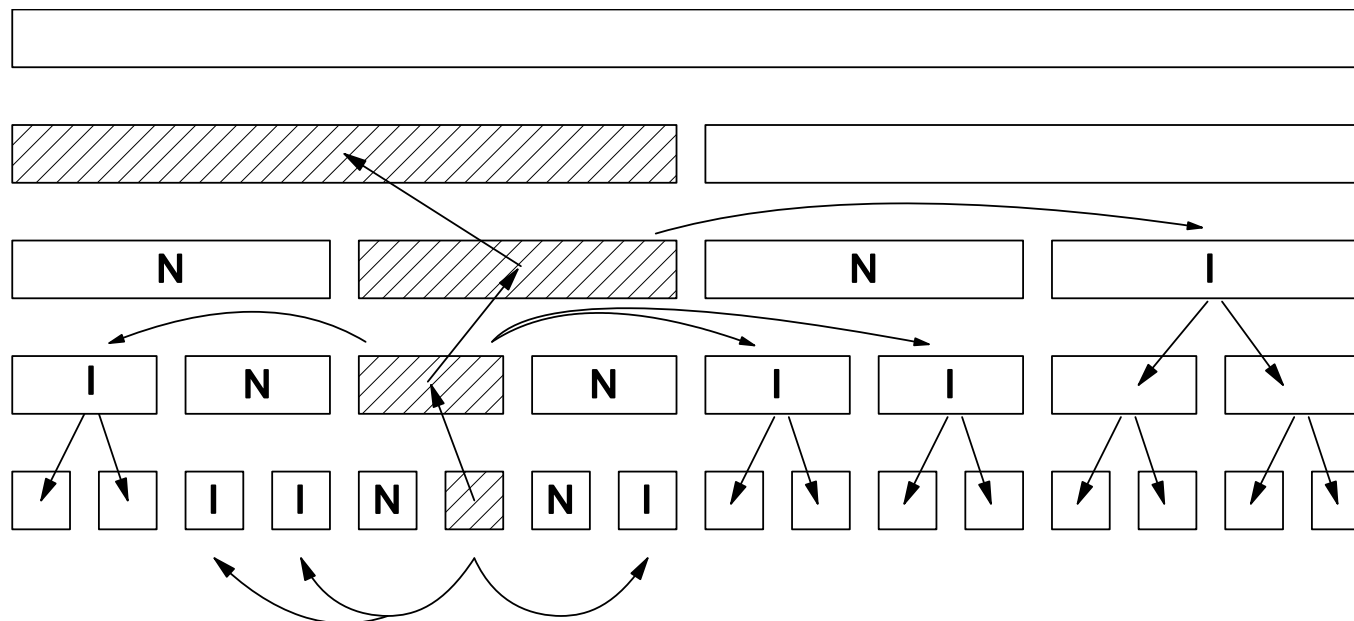
⇒ Hierarchical tree (levels $\ell = 0, \dots, m$) of element clusters (diameter d_ℓ)

Nearfield N: Distance $D < c d_\ell/2$

Interaction list I: $c d_\ell/2 < D < c d_{\ell-1}/2$

Algorithm:

- nearfield is evaluated directly by standard BEM
- farfield signature is transformed to the interaction list using translation operators M_L and shifted to father cluster
- downward pass of entries in the interaction lists, recovering of solution at integration points



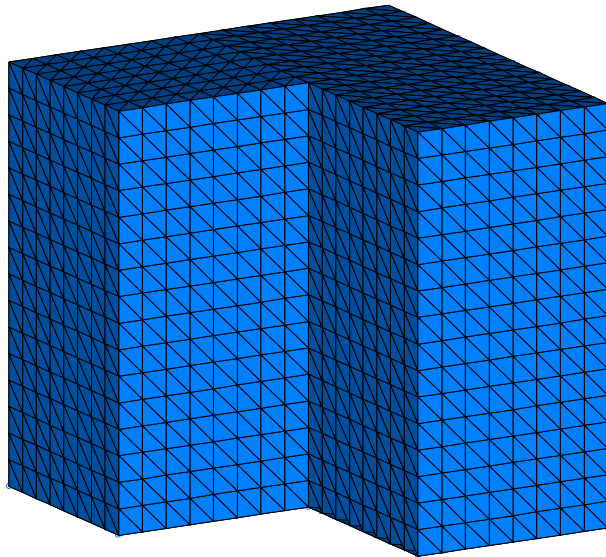
Numerical cost for $kh = \text{const} \Rightarrow$ constant error in engineering practice

Required **expansion length** $L_\ell = kd_\ell + p \ln(kd_\ell + \pi)$

Integration on unit sphere \mathbb{S}^2 : $2L_\ell^2$ quadrature points $\Rightarrow 2L_\ell^2$ coefficients for $F(s)$

- **Application of translation operator** M_L
- **Interpolation scheme** for shift of farfield representation $F(s)$ to father cluster
 - Conversion of farfield representation $F_\ell(s)$ to multipole coefficients
Algorithm based on FFT: L_ℓ FFTs of length $2L_\ell$
 $2L_\ell$ 1D multipole expansions of length L_ℓ
 - Adding zeros in original multipole expansion
 - Conversion of multipole coefficients to farfield representation $F_{\ell-1}(s)$
 - Translation of $F_{\ell-1}(s)$ to new center
- **Nearfield computation**
 - Nearfield size $\sim \log^2 N$ for each cluster

\Rightarrow Numerical cost for total cluster tree $\mathcal{O}(N \log^2 N)$



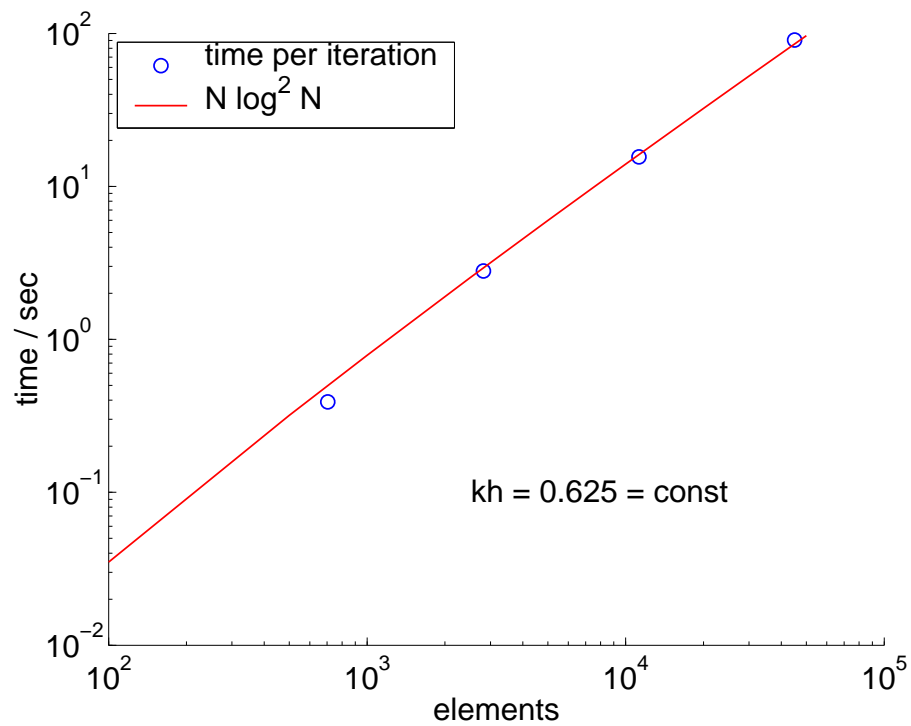
L-Shape domain 1 m x 1 m x 1 m,
monopole source applied inside,
analytical Neumann data is boundary condition,
exterior acoustic problem,
10 elements per wave length.

Preconditioning with single layer potential.

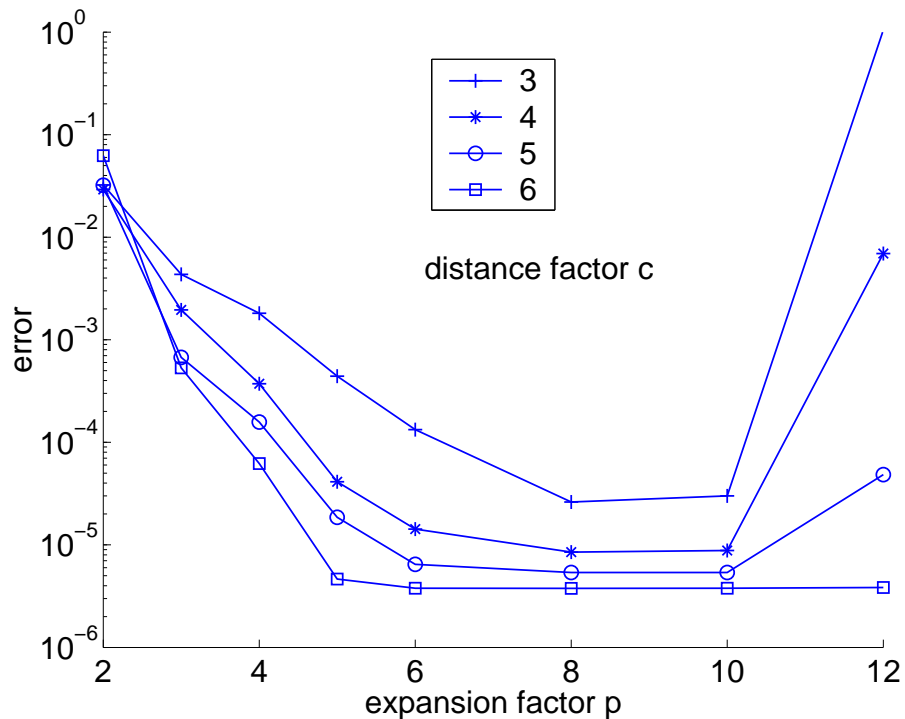
Distance factor $c = 4$, expansion factor $p = 2$.

elements	h	k	t_{near}	iterations	$t / \text{iteration}^*$	Dir error
704	0.125 m	5 m^{-1}	16.7 s	21	0.4 s	0.09
2816	0.063 m	10 m^{-1}	60.2 s	66	2.8 s	0.04
11264	0.031 m	20 m^{-1}	226 s	163	16 s	0.03
45056	0.016 m	40 m^{-1}	1012 s	452	90 s	0.08

$N \log^2 N$ Complexity



Predicted complexity $N \log^2 N$



Hypersingular operator evaluated on
L-shape ($k = 5 \text{ m}^{-1}$)

For cluster diameter d

Distance factor c

$$\text{Nearfield: } D < c \frac{d}{2}$$

Expansion factor p

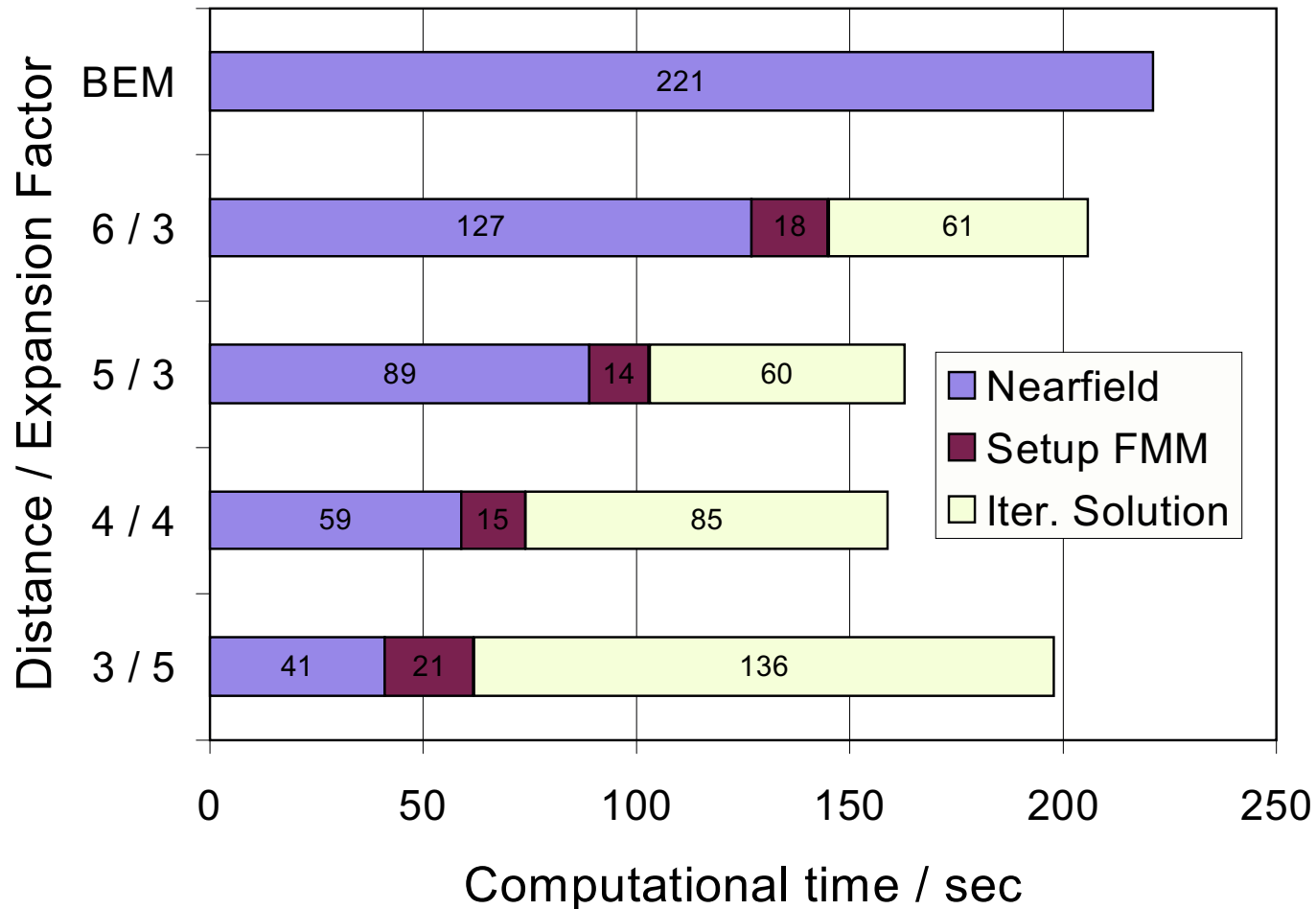
$$L = kd + p \ln(kd + \pi)$$

- Instability of multipole expansion no concern for engineering accuracies.
- Faster convergence of multipole expansion for larger near-field.
- Choice of distance and expansion factors determines efficiency of algorithm.

Efficiency of Multipole-BEM

Computing time for L-shape, 2816 elements , $k = 5 \text{ m}^{-1}$

Parameters chosen to yield error $< 10^{-3}$ compared to standard BEM



Fine meshes and high frequencies in Multipole-BEM simulations yield ill-conditioned systems of equations and high iteration counts.

High iteration counts are expensive

- Multipole algorithm carried out for each iteration
- Good convergence of GMRES without restart, only, need to store each iterate

$$\Rightarrow \text{Solve: } P^{-1}Ax = P^{-1}b$$

Requirements for preconditioner P

- Low condition number $\kappa(P^{-1}A)$
optimum: $\kappa(P^{-1}A) = \text{const}$, independent of mesh size and frequency
- Application of P^{-1} with numerical cost of at most $\mathcal{O}(N \log^2 N)$

Basic idea

Operator splitting $A = A_0 + \tilde{A}$ with A_0 bounded.

Eigenvalues of $A_0^{-1}A = I + A_0^{-1}\tilde{A}$ cluster at 1.

⇒ improved convergence of iterative solver.

Construction of A_0 for hyper-singular operator

$$(Du)(y) = - \int_{\Gamma_0} \frac{\partial^2 U^*(x, y)}{\partial n_x \partial n_y} u(x) ds_x - \int_{\tilde{\Gamma}} \frac{\partial^2 U^*(x, y)}{\partial n_x \partial n_y} u(x) ds_x$$

Two element layers is a reasonable choice for Γ_0 .

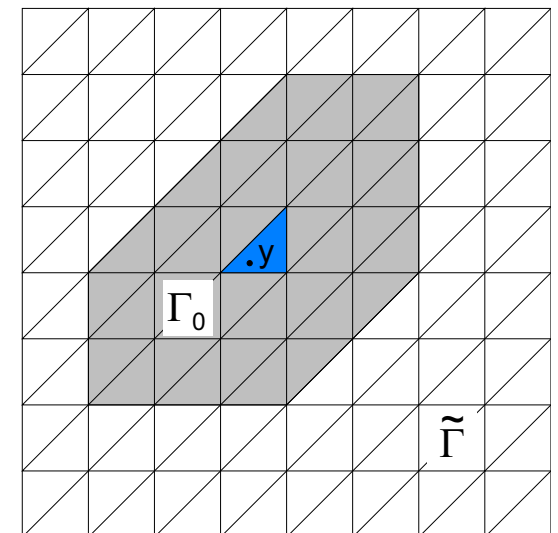
⇒ A_0 is a sparse matrix, but how to compute A_0^{-1} ?

Approximate inverse preconditioner

Minimize $\|I - A_0 P^{-1}\| \Rightarrow P^{-1} \rightarrow A_0^{-1}$

Column-oriented algorithm,

minimize $\|\underline{e}_j - A_0(P^{-1})_j\|$ separately



Based on **spectral equivalence inequality**

$$c_1(Pu, u) \leq (Au, u) \leq c_2(Pu, u)$$

which guarantees $\kappa(P^{-1}A) < \frac{c_2}{c_1}$.

From the **Calderon projector** one finds the relations

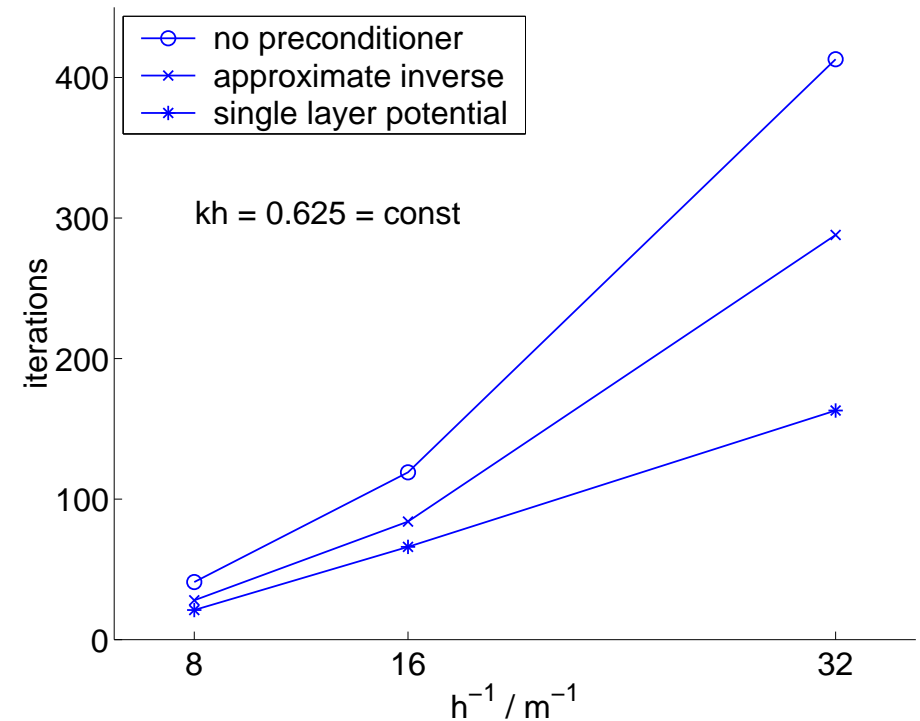
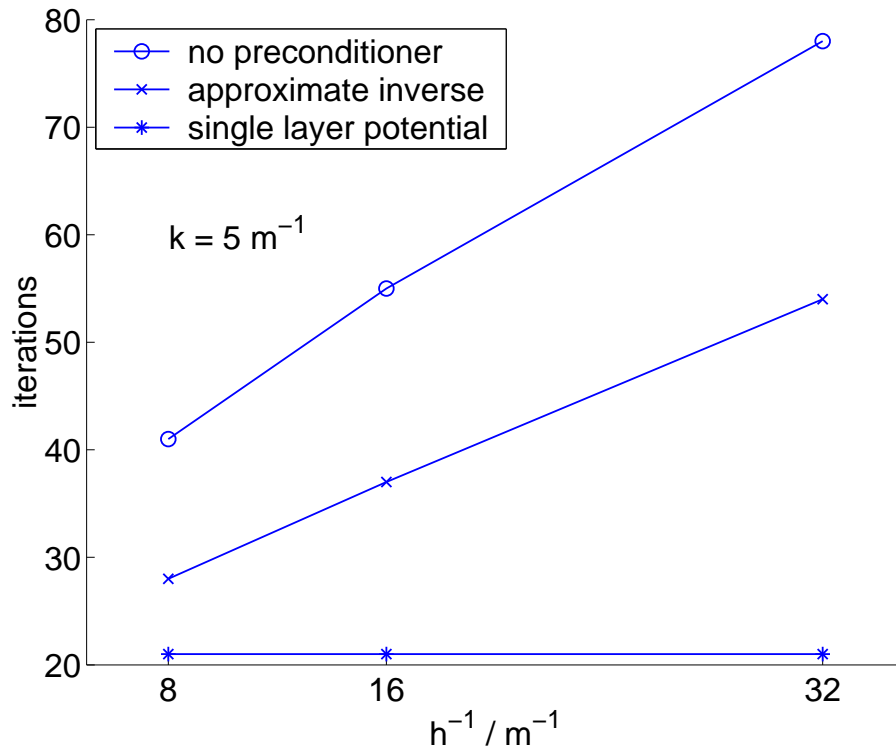
$$VD = \frac{1}{4}I - K^2, \quad DV = \frac{1}{4}I - (K')^2,$$

suggesting the single layer potential as an efficient preconditioner for the hyper singular operator.

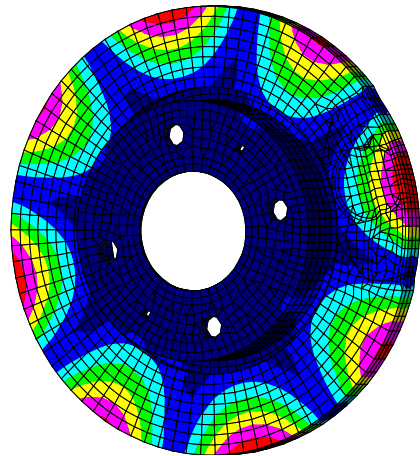
The **preconditioner matrix** is found as [Steinbach and Wendland 98]

$$P^{-1} = M^{-T}VM^{-1}.$$

Preconditioner requires application of the single layer potential V and, twice, the inverse of the mass matrix M . \Rightarrow Same complexity as matrix-vector product.

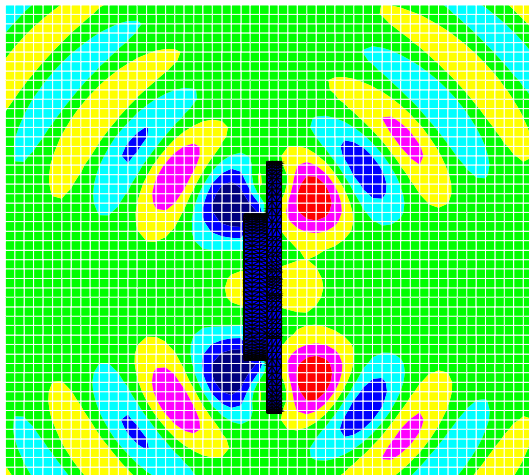


- high iteration counts for fine meshes and high frequencies
- approximate inverse preconditioner
 - reduces iteration count by a third, very cheap numerical cost
- preconditioning using single layer potential
 - suppresses influence of mesh size, still strong influence of frequency



Model of disk brake for FEM modal analysis,
normal velocity of 12th eigenmode at 3720 Hz.

Multipole-BEM simulation of acoustic field,
4422 triangular elements,
computational time nearfield matrix 10 min.



GMRES, residuum 10^{-3}

preconditioner	iterations	time for solution
without	326	29 min
approximate inverse	203	19 min
single layer potential	99	18 min

- Galerkin BEM for acoustic simulation.
- Fast multilevel multipole algorithm.
- Preconditioners for improved efficiency.

Outlook

- Preconditioners that reduce influence of wave number.
 - Current Master thesis: Multilevel Preconditioners for the Multipole BEM in Acoustics.
- Use of fast multipole BEM for acoustic–structure interaction.
 - Mortar coupling and efficient solution of the saddle point problem.